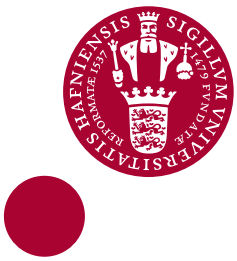

Alpha7 nicotinic acetylcholine receptors and neural network synaptic transmission in human induced pluripotent stem cell-derived neurons

Larsen, Hjalte M.; Hansen, Susanne K.; Mikkelsen, Jens D.; Hyttel, Poul; Stummann, Tina C.

Published in:
Stem Cell Research

DOI:
10.1016/j.scr.2019.101642

Publication date:
2019

Document version
Publisher's PDF, also known as Version of record

Stem Cell Research 41 (2019) 101642

Contents lists available at ScienceDirect

Stem Cell Research

journal homepage: www.elsevier.com/locate/scr

Alpha7 nicotinic acetylcholine receptors and neural network synaptic transmission in human induced pluripotent stem cell-derived neurons

Hjalte M. Larsen[a], Susanne K. Hansen[a], Jens D. Mikkelsen[b], Poul Hyttel[a], Tina C. Stummann[c,*]

[a] Stem Cells and Embryology Group, Department of Veterinary and Animal Sciences, Faculty of Health and Medical Sciences, University of Copenhagen, Denmark,
[b] Neurobiology Research Unit, University Hospital Copenhagen, Rigshospitalet, Denmark
[c] H. Lundbeck A/S, Ottiliavej 9, Valby, Denmark

ARTICLE INFO

Keywords:
Alpha7 nicotinic acetylcholine receptor
Human induced pluripotent stem cell derived neurons
Allosteric modulation
Synaptic transmission

ABSTRACT

The α7 nicotinic acetylcholine receptor has been extensively researched as a target for treatment of cognitive impairment in Alzheimer's disease and schizophrenia. Investigation of the α7 receptor is commonly performed in animals but it is critical to increase the biologically relevance of the model systems to fully capture the physiological role of the α7 receptor in humans. For example most humans, in contrast to animals, express the hybrid gene CHRFAM7A, the product of which modulates α7 receptor activity. In the present study, we used human induced pluripotent stem cell (hiPSC) derived neurons to establish a humanized α7 model. We established a cryobank of neural stem cells (NSCs) that could reproducibly be matured into neurons expressing neuronal markers and CHRNA7 and CHRFAM7A. The neurons responded to NMDA, GABA, and acetylcholine and exhibited synchronized spontaneous calcium oscillations. Gene expression studies and application of a range of α7 positive allosteric modulators (PNU-120595, TQS, JNJ-39393406 and AF58801) together with the α7 agonist PNU-282987 during measurement of intracellular calcium levels demonstrated the presence of functional α7 receptors in matured hiPSC-derived neuronal cultures. Pharmacological α7 activation also resulted in intracellular signaling as measured by ERK 1/2 phosphorylation and c-Fos protein expression. Moreover, PNU-120596 increased the frequency of the spontaneous calcium oscillations demonstrating implication of α7 receptors in human synaptic networks activity. Overall, we show that hiPSC derived neurons are an advanced in vitro model for studying human α7 receptor pharmacology and the involvement of this receptor in cellular processes as intracellular signaling and synaptic transmission.

1. Introduction

Development of pharmaceuticals for treatment of neurological diseases e.g. Alzheimer's disease and schizophrenia, is a challenging task due to the complexity of the diseases, lack of translational in vivo and in vitro models, and limited access to human brain material (Dragunow, 2008; Kesselheim et al., 2015; Selkoe, 2011). Cognitive impairments in form of reduced attention, learning, and working memory are frequent symptoms in both diseases. Investigations in Alzheimer's disease models have shown several dysfunctional receptor systems affecting the basal forebrain, pre-frontal cortex, and hippocampus (reviewed in Millan et al., 2012). The α7 nicotinic acetylcholine (α7) receptor, an ionotropic receptor channel highly permeable to calcium and enriched in areas of the hippocampus and cortex (Breese et al., 1997; Court et al., 1997; Freedman et al., 1993), has been broadly studied as a potential drug target for treatment of cognitive dysfunction in Alzheimer's disease and schizophrenia (Hashimoto et al., 2008; Haydar and Dunlop, 2010; Levin et al., 2006, 2002; Toyohara and Hashimoto, 2010). α7 receptor function can be modulated by partial agonists (Biton et al., 2007; Lieberman et al., 2013; Prickaerts et al., 2012) as well as positive allosteric modulators (PAMs) (Eskildsen et al., 2014; Hurst et al., 2005; Krause et al., 1998; Timmermann et al., 2007). PAMs are compounds that bind to the receptor at sites distinct from the orthosteric site and enhance the activation amplitude (type I and II) or diminish desensitization (type II), but show no agonist activity themselves (Grønlien et al., 2007). Indeed, α7 PAMs have shown to improve memory and cognitive function in vivo and are considered cognitive enhancers (Thomsen et al., 2010a; Timmermann et al., 2007; Williams et al., 2011).

Studies in adult rat hippocampus have demonstrated the presence of both pre- and post-synaptic α7 receptors (Fabian-Fine et al., 2001). Presynaptic receptor activation promotes local depolarization, which

* Corresponding author.
E-mail address: tcst@lundbeck.com (T.C. Stummann).

https://doi.org/10.1016/j.scr.2019.101642
Received 9 July 2019; Received in revised form 9 October 2019; Accepted 28 October 2019
Available online 31 October 2019

enhances the probability of neurotransmitter release into the synapses and thereby signal conductance to adjacent neurons (Thomsen et al., 2010a). In line, presynaptic α7 receptors has been reported to modulate both GABA (Alkondon et al., 2000; Alkondon and Albuquerque, 2001) and glutamate (Cheng and Yakel, 2014; Gray et al., 1996; Sharma et al., 2008) synaptic transmission in the hippocampus. Activation of post-synaptic α7 receptors initiate downstream pathways including phosphorylation of the MAP kinase ERK (Dajas-Bailador et al., 2002b; Dineley et al., 2001; El Kouhen et al., 2009) and expression of proto-onco gene c-Fos protein (Hansen et al., 2007; Thomsen et al., 2010a, 2010b). Noticeably, embryonic α7 subunit expression is increased compared to the adult stage (Adams et al., 2002; Falk et al., 2003), suggesting also a developmental role of the receptor in neuronal proliferation and synapse establishment (Court et al., 1997).

The discovery of human induced pluripotent stem cells (hiPSCs) was a hallmark in modern biology offering the ability to derive a whole range of somatic cell types (Takahashi et al., 2007; Yu et al., 2007). Importantly, this also provided a renewable source of human neurons, which facilitated humanized in vitro modelling of neurodegenerative and psychiatric diseases such as sporadic and familial Alzheimer's disease (Israel et al., 2012; Muratore et al., 2014) and schizophrenia (Brennand et al., 2011). hiPSC-derived neurons provide a promising alternative to immortalized cell lines and non-human primary neuronal cultures for studying the α7 receptor in a human neuronal cellular background with native genome and proteome. For example, most humans have one or two copies of the CHRFAM7A gene consisting of a partial duplication of the α7 gene (CHRNA7) fused to a copy of the FAM7A gene. This gene combination is only expressed in humans and CHRFAM7A expression reduces ACh evoked α7 currents (Araud et al., 2011). Moreover, α7 receptor activation increases intracellular calcium influx though the α7 receptor channel, but also by secondary downstream effects such as influx via L-type voltage-gated calcium channels and from IP3 and ryanodine receptor guarded intracellular stores (Dajas-Bailador et al., 2002a; Guerra-Álvarez et al., 2015). Such interactions with other cellular mechanisms must be better reflected using neuronal models with endogenously expressed α7 receptor.

Upon neural differentiation, hiPSC-derived neurons express α7 receptors, develop synaptic connections and display spontaneous action potentials and calcium oscillations (Gill et al., 2013; Hansen et al., 2016; Israel et al., 2012; Muratore et al., 2014). In this study, we link the α7 receptor expression in hiPSC-derived neurons to relevant cellular processes as intracellular signaling and synaptic transmission by (1) characterizing the native expression of the α7 receptor complex in hiPSC-derived neurons, (2) addressing if α7 stimulation result in activation of relevant cellular downstream processes, (3) characterizing the hiPSC-derived neurons as a model for synaptic transmission, and finally (4) investigating the involvement of the α7 receptor in synaptic transmission. The overall aims were to develop a model for studying A) α7 receptor pharmacology in a human context and B) the role of α7 receptors in cellular processes as intracellular signaling and synaptic networks activity.

2. Materials and methods

2.1. Compounds

AF58801 (Eskildsen et al., 2014), Cx516, diazepam, and PNU-282987 were synthesized at H. Lundbeck A/S at chemical grade with a purity of >90%. 4-AP (275875), Acetylcholine (A6625), atropine (A0257), ifenprodil (I2892), ketamine (K2753), mecamylamine (M9020), MK-801 (M107), nicotine (N5260), and PNU-120596 (P0043) were purchased from Sigma-Aldrich (Brøndby, Denmark). TQS was synthesized by Chembridge Corporation (San Diego, CA, USA) and JNJ-39393406 by WuXi (Shanghai, China). 2-APB (1224), bicuculline (2503), methyllycaconitine (1029), QNZ46 (4801), ryanodine (1329), TCN237 (4072), and tetrodotoxin citrate (1069) were purchased from Tocris bioscience (Bristol, UK). ω-Conotoxin GVIA (H-6615) and MVIIA (H-8210) were purchased from Bachem (Bubendorf, Switzerland). Single doses where picked based on typical concentrations used in other cell-based studies (in-house experience and literature data).

2.2. hiPSC generation, NSC differentiation, and NSC banking

Three hiPSCs clones (NHDF K1_shp53, K2_shp53, and K3_shp53 deposited in the European Bank of induced Pluripotent Stem Cells (EBiSC) as BIONi010-A, BIONi010-B and BIONi010-C) from a healthy 18y male were generated and differentiated into neural stem cells (NSCs) and master cryostocks were frozen at passage 2 (day 16–19) as previously described (Hansen et al., 2016; Rasmussen et al., 2014). Master cryostocks were thawed and cultured for two passages (10 days) for establishment of a working cryobank. During generation of the working cryobank, the NSCs were cultured in neural expansion medium (NEM) consisting of 50% Advanced DMEM/F-12 (Thermo Fisher Scientific, 12634), 50% Neurobasal medium (Thermo Fisher Scientific, 21103–049), 2% Neuronal induction supplement (Thermo Fisher Scientific, A16477- 01), and 0.1% PenStrep (Thermo Fisher Scientific, 15140–122) on plates coated with 10 μg/cm^2 poly- L-ornithine (Sigma-Aldrich, P3655) and 1 μg/cm^2 laminin (Sigma-Aldrich, L2020) referred to as PLO/lam-coating at 37 °C (5% CO_2, 95% humidity).

2.3. NSCs and maturation

The NSC maturation protocol is illustrated in Fig. 1A. NSC working cryostocks (passage 4) were thawed and expanded in NEM for two days in PLO/lam-coated 6-well plates. NSCs were split (defined as day 0) using 10 min accutase (Thermo Fisher Scientific, A11105) treatment and plated at a density of 1.6E6 cells/6-well and matured in neural maturation medium (NMM) consisting of 50% DMEM-F12 (Thermo Fisher Scientific, 31331–028), 50% Neurobasal medium (Thermo Fisher Scientific, 21103–049), 0.5% N2 (Thermo Fisher Scientific, 17502–048), 0.5% B27 (Thermo Fisher Scientific, 17504–044), 0.5 mM GlutaMAX supplement (Thermo Fisher Scientific, 35050–061), 0.5% NEAA supplement (Thermo Fisher Scientific, 11140–050), 50 μM 2-mercaptoethanol (Thermo Fisher Scientific, 21985023), 2.5 μg/mL insulin (Sigma-Aldrich, 19278) supplemented with maturation factors: 20 ng/mL BDNF (R&D Systems, 248-BD), 10 ng/mL GDNF (R&D Systems, 212-GD), 200 μM L-Ascorbic Acid (Sigma-Aldrich, A5960), and 500 μM db-cAMP (Sigma-Aldrich, D0627). After 8/9 days in NMM, the cells were seeded in 96-well plates at a density of 50,000 cells/well (166,700 cells/cm^2) and further matured in NMM medium for 2–5 weeks. Medium containing maturation factors was used within a week and changed every second day. 10 μM ROCK inhibitor (Sigma-Aldrich, Y0503) was added overnight upon thawing and splitting. The ages of the hiPSC neurons used in the different experiments are given as days or weeks of culturing in NMM.

2.4. Immunocytochemistry

Cells seeded in PLO/lam-coated Cell Carrier (Perkin Elmar, 6005550) plates were fixed in 4% paraformaldehyde for 15 min at room temperature, blocked in KPBS (10 mM phosphate buffer, 150 mM NaCl, and 3.4 mM KCl) supplemented with 0.5% BSA, 0.1% triton X-100, and 5% normal swine serum (Jackson ImmunoResearch, 014–000–121) for 20 min and incubated in blocking buffer containing primary antibody overnight (4 °C) (listed in Supplementary). Subsequently, the samples were incubated with secondary antibodies (listed in Supplementary) and 0.67 ug/mL Hoechst 33342 (Invitrogen, H1399) for 1 h at room temperature, mounted in Prolong Gold Antifade Mountant (Thermo Scientific, P36934), and visualized on Leica DM5500 B (Leica, DE).

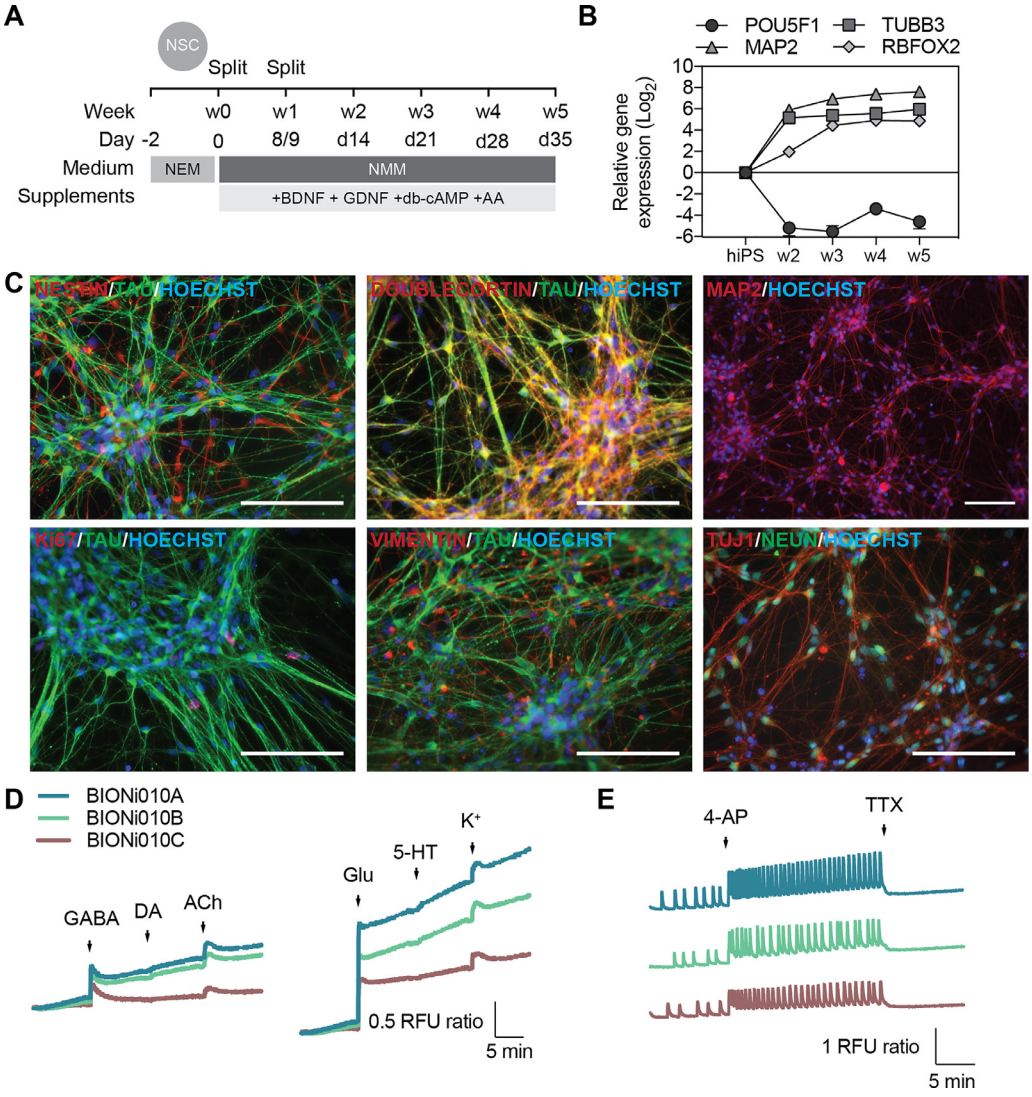

Fig. 1. Maturation of hiPSC-derived NSCs to spontaneously active neurons. **A:** NSC maturation protocol used for differentiation of spontaneously active neurons. Protocol is depicted with time points, medium, and supplements. **B:** q-PCR for gene expression of pluripotency marker Oct-4 (POU5F1, $P < 0.0001$ day 14–35 compared to day 0), neuronal markers βIII-tubulin (*TUBB3,* $P < 0.05$ day 14–21, $P < 0.001$ day 28 and $P < 0.0001$ day 35 compared to day 0) and microtubule associated protein-2 (*MAP2,* $P < 0.05$ day 14, $P < 0.001$ day 21 and $P < 0.0001$ day 28–35 compared to day 0), and post-mitotic neuron marker NeuN (*RBFOX2,* $P < 0.01$ day 21 and $P < 0.001$ day 28–35 compared to day 0) at different stages of differentiation (mean ± SEM, $n = 3$, $m = 4$). **C:** Immunocytochemistry of the hiPSC-derived neurons showing protein expression of neuroprogenitor markers nestin and vimentin, cell proliferation marker Ki67, neuronal markers doublecortin, βIII-tubulin (TuJ1), MAP2, and Tau, and NeuN. Scale bars: 100 µm (d21, $n = 3$, $m = 1$, exemplified with BIONi010A) **D:** Changes in intracellular calcium following application of 100 µM GABA, 100 µM dopamine (DA), 300 µM acetylcholine (ACh), 300 µM glutamate (Glu; + 10 µM glycin), 100 µM serotonin (5-HT), 25 mM potassium chloride (K^+) (mean for each n, d21-22, $n = 3$, $m = 4$). **E:** Effect of 250 µM 4-AP followed by 1 µM TTX on neuronal calcium oscillations (representative traces are shown for each line, d28, $n = 3$, $m = 4$).

2.5. Quantitative real time PCR (qPCR)

SYBR Green Cell-to-CT kit (Ambion, 4402957) was used for RNA isolation and reverse transcription to cDNA. 4x diluted cDNA was used as template for qPCR with TaqMan® Fast Advanced Master Mix and TaqMan primers purchased from Thermo Scientific (listed in Supplementary). The ΔΔ-CT method was applied to expression data and individual genes normalized to geometric mean of housekeeping genes (RPL13A, GUSB, and HSP90AB1), and mean of undifferentiated hiPSC cDNA samples from all three lines.

2.6. Intracellular calcium measurements

Neurons were loaded for 1 h at room temperature with Calcium-4 dye (Molecular Devices, R8141) dissolved in assay buffer (HBSS w/o Ca^{2+}/Mg^{2+}, 20 mM HEPES (Sigma-Aldrich, H4034), 3 mM CaCl). Image based measurement of cytosolic calcium kinetics (excitation and emission wavelengths of 480, and 540 nm, respectively) and compound applications were conducted using the FDSS7000 system (Hamamatsu, Japan). The instrument readout is the total fluorescent intensity per well in relative fluorescence units (RFU), which are reported as ratio to the first sampling data point and termed "RFU ratio" throughout the manuscript. Dimethyl sulfoxide (DMSO) assay concentration was maintained at ≤0.5% and kept constant within different conditions of the same experiments. The FDSS application paradigm used in experiments shown in Figs. 2D, 2E, 2F, 2G, 3A and 3B is illustrated in Fig. 2C, except that in Fig. 2G a 30 min preincubation with inhibitor was included in the experiment. 25 mM KCl application was included in a set of wells on all plates as plate to plate calibrator. Experiments were performed at room temperature. FDSS7000Ex/uCell software was used to quantify the maximum RFU ratio upon agonist application, where after vehicle values were subtracted and data were normalized to the mean maximum ratio upon KCl stimuli. The Data in Fig. 2G was additionally normalized to the response to PNU282987 + PNU120596 in the absence of inhibitor. Calcium oscillations recordings were performed at 37 °C. FDSS data shown in Fig. 4 were done as 20 min measurement of spontaneous calcium oscillations (baseline activity) and 20 min measurements in the presences of pharmacological treatments. The number of peaks and the mean peak amplitudes in the 20 min intervals were quantified using FDSS7000Ex/uCell combined with FDSS Waveform Analysis software. Data from individual wells were normalized to their baseline values (as well-to-well normalizer) and to mean of vehicle control.

2.7. Western blotting

Neurons were washed, and assay buffer added 3 h prior to stimulation. Stimulation compounds were diluted in assay buffer. For phosphorylation of ERK neurons were incubated for 5 min (37 °C) and for c-Fos 1 h (37 °C). Neurons were harvested in DPBS (w/o Mg^{2+}/Ca^{2+})

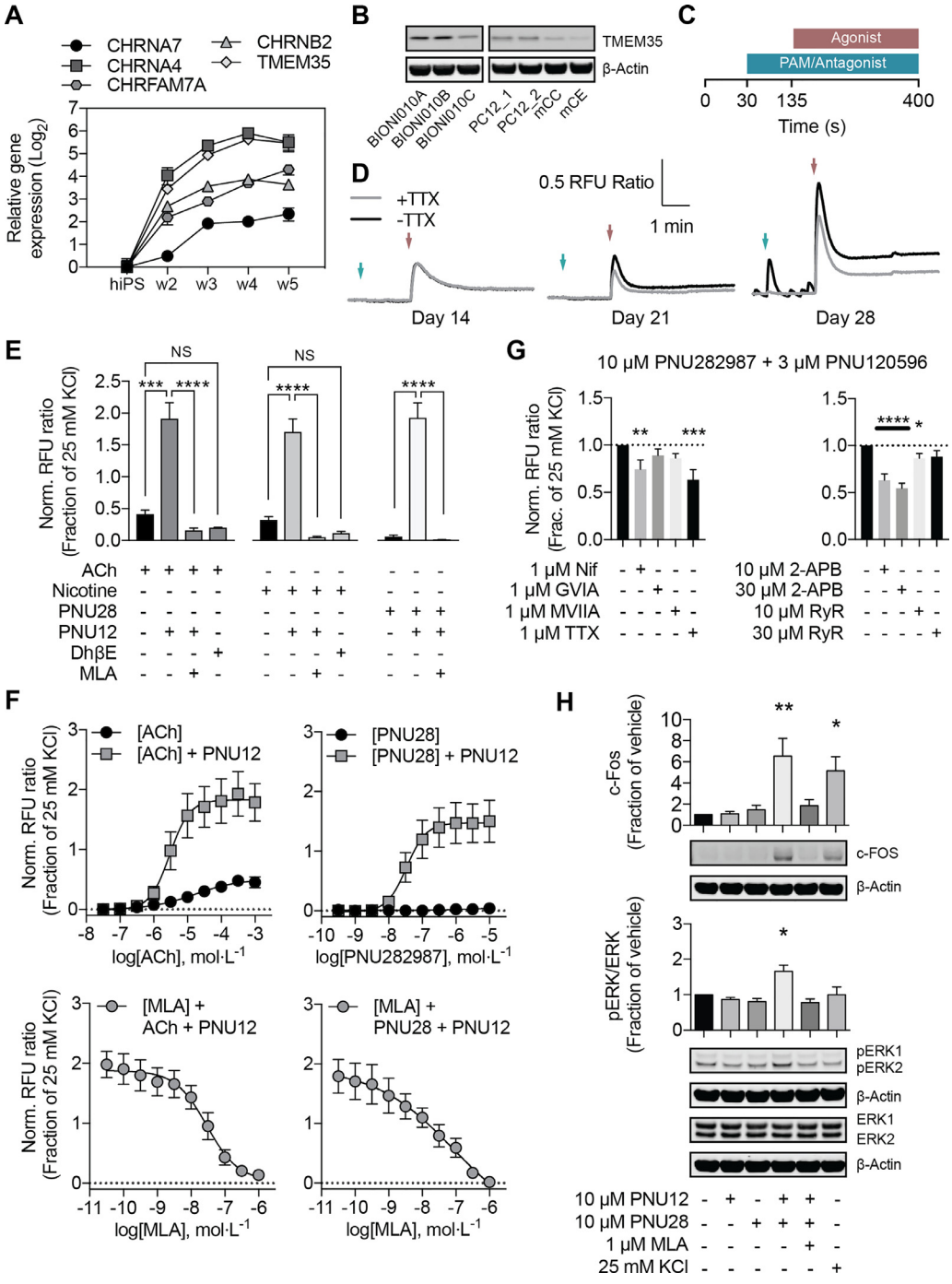

Fig. 2. hiPSC-derived neurons express functional α7 receptors.

A: q-PCR for gene expression of nAChR subunits α7 (*CHRNA7,* $P < 0.01$ week 3–4 and $P < 0.001$ week 5 compared to day 0), α4 (*CHRNA4,* $P < 0.01$ week 3 + 5 and $P < 0.001$ week 4 compared to day 0), β2 (*CHRNB2,* $P < 0.05$ day 14 and $P < 0.0001$ week 3–5 compared to day 0), hybrid α7 (*CHRFAM7A,* $P < 0.05$ week 3, $P < 0.001$ week 4 and $P < 0.0001$ week 5 compared to day 0), and chaperone transmembrane protein 35A (*TMEM35,* $P < 0.01$ week 3, $P < 0.0001$ week 4 and $P < 0.001$ week 5 compared to day 0) at different stages of neuronal differentiation (mean ± SEM, $n = 3$, $m = 4$). **B:** Western blot of TMEM35 in d21 hiPSC-derived neurons, PC12 cells, mouse cerebrum (mCC), and cerebellum (mCE) ($n = 1$, $m = 1$). **C:** Compound application paradigm used in 2D, 2E, 2F, 2 G. **D:** Calcium traces showing α7 stimulation (3 μM PNU-120596 plus 10 μM PNU-282987) in the presence or absence of 1 μM TTX. Arrows indicate additions outlined in "C" (mean, $n = 3$, $m = 4$). **E:** Change in intracellular calcium following stimulation with 100 μM acetylcholine (ACh), 25 μM nicotine, and 10 μM PNU-282987 alone or in the presence of 3 μM PNU-120596, 1 μM MLA or 10 μM DhβE (mean ± SEM, d21-22, $n = 3$, $n = 2$–4). The experiments were done in the presence of TTX. **F:** Concentration-dependent activation of α7 with ACh and PNU-282987 in the presence and absence of 3 μM PNU-120596, and concentration-dependent inhibition of α7 with antagonist MLA (mean ± SEM, d21, $n = 3$, $n = 4$). The experiments were done in the presence of TTX. **G:** Effects of inhibiting voltage-gated channels or calcium release from intracellular calcium stores on α7 evoked cytosolic calcium. Neural cultures were pre-incubated with channel blockers (1 μM nifedipine, 1 μM w-CTx GVIA, 1 μM w-CTx MVIIA, or 1 μM TTX) or blockers of calcium release from intracellular calcium stores (10–30 μM 2-APB, or 10–30 μM ryanodine) 30 min prior to α7 stimulation with 3 μM PNU120596 and 10 μM PNU-282987 (mean ± SEM, d20-23, $n = 3$, $m = 4$). The experiments were done in the presence of TTX **H:** Western blot of pERK/ERK (sum of pERK and ERK1/2) and c-Fos following α7 stimulation with indicated compounds (mean ± SEM, d23-26, $n = 3$, $n = 2$). Representative blots are shown below graphs. **All figure panels:** Statistical significance was determined using one-way ANOVA followed by post hoc Dunnett's or Sidak's multiple comparison test; $^{*}P < 0.05$, $^{**}P < 0.01$, $^{***}P < 0.005$.

containing protease and phosphatase inhibitor cocktail (Roche, 11697498001, 04906837001), centrifuged (1000xg, 10 min, 4 °C), and lysed for 30 min in RIPA buffer (Sigma-Aldrich, R0278) supplemented with inhibitor cocktail. Lysate was centrifuged (18.000xg, 20 min, 4 °C), and the supernatant was collected and stored at −80 °C. Protein concentration was determined using Pierce BCA (Thermo Scientific, 23,225). Samples were mixed with loading buffer to a final concentration of 100 mM DDT, 1x NuPAGE LDS sample buffer (Thermo Scientific, NP0007) and incubated at 95 °C for 5 min. 10 μg protein was loaded in 15 wells NuPAGE Novex 4–12% Bis-Tris protein gels (Thermo Scientific, NP0323) with Chameleon Duo protein ladder (LI-COR, 928–6000). Electrophoresis was done at 200 V with variable power and electrical current for 45 min on ice. Gel was blotted to nitrocellulose membrane (Thermo Scientific, IB23001) using iBlot 2 dry blotting (Thermo Scientific, IB21001). Nitrocellulose membrane was blocked in blocking buffer (1:1 LI-COR, 927–40,000 and DPBS) for 30 min with shaking. Primary antibodies (listed in Supplementary) were diluted in blocking buffer and incubated overnight at 4 °C on a rotating table. Following 6 washes (30 min) in DPBS + 0.1% tween, membranes were incubated with secondary antibodies diluted in secondary buffer (DPBS,

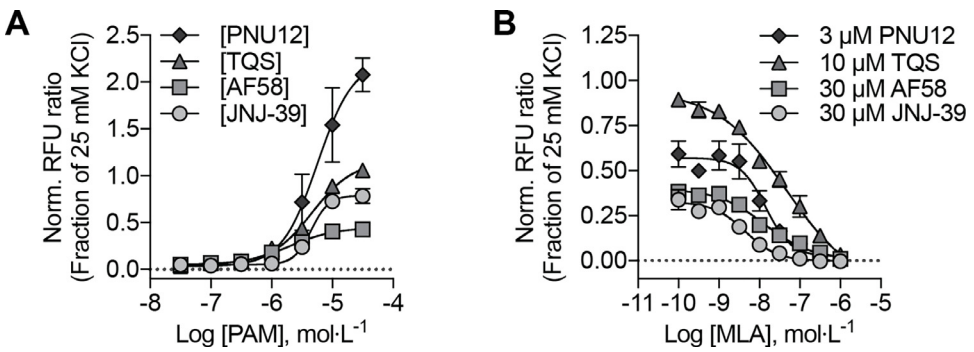

Fig. 3. Chemically diverse α7 positive allosteric modulators show concentration-dependent activation of α7.
A/B: Concentration-response of α7 positive allosteric modulators (type 2: PNU-120596 (PNU12), TQS, type 1/2: AF58801 (AF58), JNJ-39393406 (JNJ-29)) and α7 receptor antagonist MLA following stimulation with 10 µM PNU- 282987 according to the paradigm shown in Fig. 2C (mean ± SEM, d21-22, $n = 3$, $m = 4$). Experiments were done in the presence of TTX.

0.1% tween, 0.02% SDS) for 1 h, washed 6 times in DPBS + 0.1% tween, and 2 times in PBS, and scanned on LI-COR Odyssey CLx. Data were extracted using Imaging Studio (LI-COR, 9140–500).

2.8. Curve fitting and statistical analysis

All data analyses were conducted in Excel (Microsoft, CA). Curve fitting and statistical analysis were done using Prism (GraphPad, La Jolla). All data are shown as mean ± SEM ("n" = individual cell lines run in independent experiments except in Fig. 2D where the lines were run in parallel, "m" = technical replicates) unless stated otherwise.

3. Results

3.1. hiPSC-derived neurons express neuronal markers, respond to neurotransmitters and show synchronized calcium oscillations

We aimed at generating a reproducible hiPSC-based system for investigating natively expressed functional α7 receptors in a system with a good throughput. From a single working stock cryovial (4×10^6 NSCs), we generate $22 \times 10^6 \pm 1 \times 10^6$ NSCs, i.e. enough for seeding three to four 96-well plates (50.000 cells/well). To account for the variance induced by fibroblast reprogramming or cell culture related factors, experiments were conducted with three hiPSC clones. We used qPCR to determine gene expression relative to undifferentiated hiPSCs, at four time points during terminal maturation of the NSCs into neurons (day 14, 21, 28, 35/36). Onset of differentiation was associated with a down-regulation of the pluripotency marker OCT4 (*POU5F1*) and an upregulation of the pan-neuronal markers, βIII-tubulin (*TUBB3*, 60-folds day 35), microtubule associated protein-2 (MAP2, 200-folds day 35/36) and NeuN (RBFOX2, 29-folds day 35/36), which all three had reached a plateau from week 3 (Fig. 1B). Immunostainings at day 21 (Fig. 1C) confirmed the presence of MAP2, βIII-tubulin, and NeuN protein and additionally showed expression of doublecortin and microtubule associated protein tau. Smaller subpopulations were positive for the neuronal progenitor markers (nestin, vimentin) and the proliferation marker Ki67.

Based on the pan-neuronal mRNA and protein marker expression in our neuronal cultures, we hypothesized that the cultures would be sufficiently mature to express several receptor classes. To address this, we investigated the effects of neurotransmitters on intracellular calcium levels (Fig. 1D). The experiments were performed in the presence of tetrodotoxin (TTX, 1 µM) to eliminate spontaneous calcium oscillations blurring the neurotransmitter responses. Intracellular calcium increased in response to the neurotransmitters γ-aminobutyric acid (GABA, 100 µM), acetylcholine (300 µM), and glutamate (300 µM). Furthermore, depolarization of the membrane potential by addition of potassium chloride increased intracellular calcium levels, most likely by opening of voltage-gated calcium channels. Neither dopamine nor serotonin had any effect on calcium levels. The calcium assay only reveals the presence of a receptor if its activation causes a calcium influx. It may be directly via the receptor or via downstream effects. Hence, the presence of dopamine and serotonin receptors cannot be excluded, even though they were not demonstrated. G protein–coupled $GABA_B$ receptors are linked to inactivation, and not activation, of voltage-gated calcium channels (Chalifoux and Carter, 2011). Therefore, the GABA effect probably reflects activation of $GABA_A$, chloride channels, resulting in membrane depolarization and secondary opening of voltage-gated calcium channels. In the adult brain, GABA is an inhibitory neurotransmitter. In the immature brain, high intracellular chloride concentrations are reported to result in depolarizing GABA responses in neurons (Succol et al., 2012). However, as the Nernst equilibrium potential for chloride is close to typical neuronal membrane potentials, experimental conditions will be highly determining for whether $GABA_A$ receptor activation induces depolarization or hyperpolarization. Whether one or the other reason explains the GABA induced calcium increase in our cultures, the data demonstrate the presence of functional GABA receptors.

Neurons from all three hiPSC clones showed the same response pattern.

In some experiments, spontaneous calcium oscillations were observed as early as week 3. Keeping the neurons in culture for one additional week resulted in consistent presence of spontaneous calcium oscillations. Coordinated synchronized network activity is required to detect oscillations in the applied calcium assay, as the readout is the total fluorescence per wells. Hence the data demonstrate synaptic connectivity in the cultures. This was further confirmed by live imaging (see Fig. S1). Application of the voltage-gated potassium channel blocker 4-aminopyridine (4-AP, 250 µM) resulted in an increase in oscillation amplitude and frequency (Fig. 1E), presumable by easing membrane potential depolarization. Addition of the voltage-gated sodium channel blocker TTX (1 µM) abolished all activity (Fig. 1E) verifying a role for action potentials in facilitation of the coordinated calcium oscillations.

3.2. hiPSC-derived neurons express functional α7 receptors

We used qPCR to examine the changes in gene expression of nicotinic acetylcholine receptor (nAChR) subunits during neuronal maturation (Fig. 2A). α4 (*CHRNA4*) showed the largest upregulation (45-folds day 35), while β2 (*CHRNB2*) (12-folds day 35), and α7 (*CHRNA7*) (5-folds day 35) expression changes were more limited. Interestingly, also the human specific hybrid α7 gene (*CHRFAM7A*) was up-regulated (20-folds day 35). The gene product is reported to co-assembles with native α7 subunits and act as a dominant negative modulator of the receptor function (Sinkus et al., 2015). This highlights the importance of using a human α7 model. We also investigated the expression of chaperone *TMEM35*, recently shown to be required for surface expression of the α7 receptor complex (Gu et al., 2016). *TMEM35* mRNA expression was up-regulated (44-folds day 35), and interestingly correlated with *CHRNA4* and *CHRNB2* expression levels (Fig. 2A). TMEM35 protein expression was confirmed by Western Blotting (Fig. 2B).

We addressed the expression of functional α7 receptors by

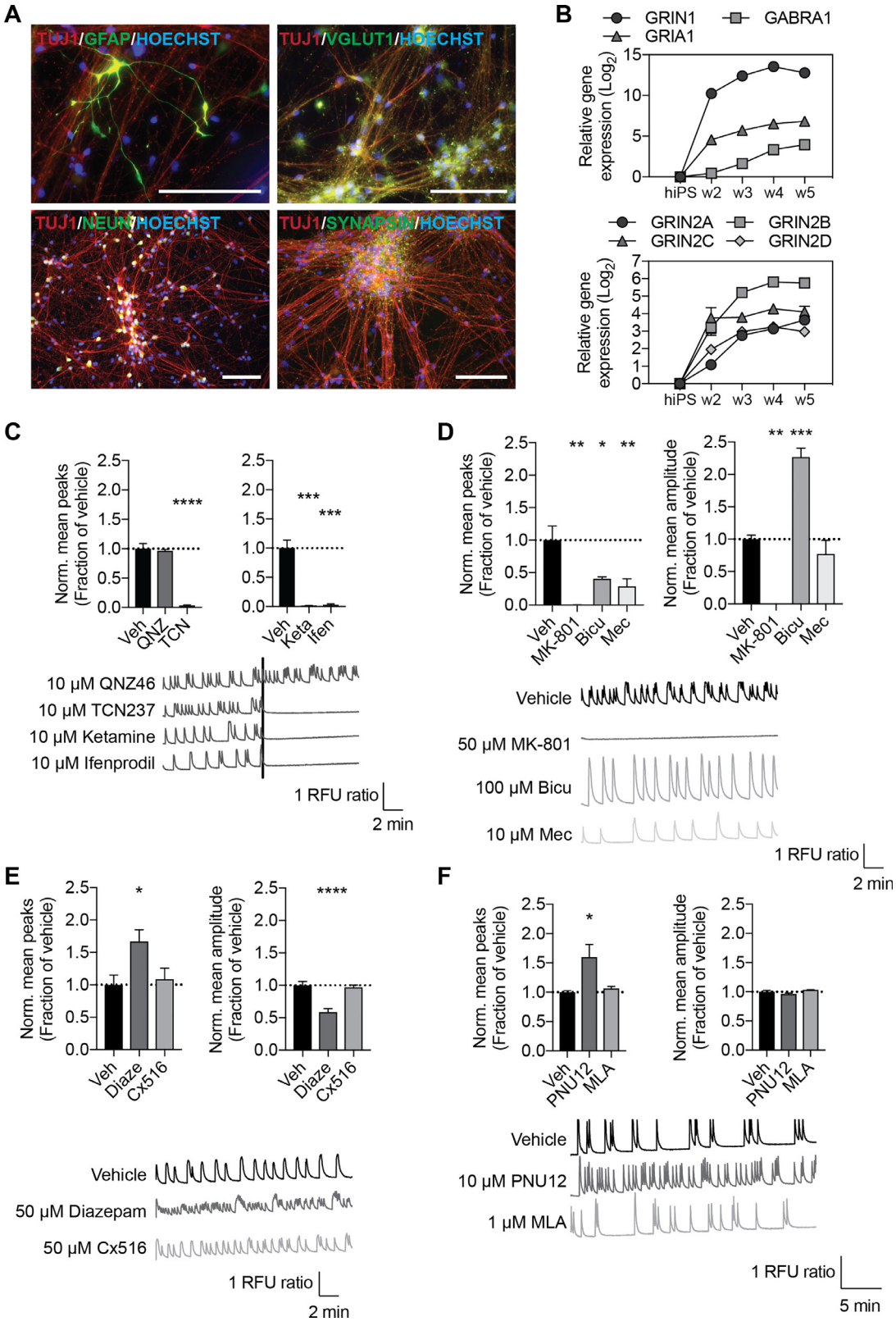

(caption on next page)

pharmacological characterization using the compound application paradigm described in Fig. 2C and assessing effects on intracellular calcium. Calcium levels increased in response to stimuli with α7 receptors type II PAM, PNU-120596 (3 µM) (Hurst et al., 2005) when combined with the selective α7 agonist, PNU-282987 (10 µM) (Hajós et al., 2005) (Fig. 2D). This was evident at all neuronal maturation timepoints, i.e. indicating functional receptor expression at week 2, 3 and 4. At week 3–4, concurrent application of TTX reduced the α7-induced calcium signal. This implies amplification of the calcium response by secondary effects dependent on voltage-gated sodium

Fig. 4. hiPSC neural networks show NMDA-mediated synchronized calcium oscillations that are modulated by α7 and GABA receptors.
A: Immunocytochemistry of astrocyte marker GFAP, glutamate transporter vGLUT, post-mitotic neuron marker NEUN, and synapse marker synapsin. βIII-tubulin (TuJ1) was used to indicate neurites. Scale bars: 100 μm (d21, $n = 3$, $m = 1$, BIONi010A shown). **B:** qPCR for gene expression of GABA (*GABRA1,* $P < 0.001$ day 21 and $P < 0.0001$ day 35 compared to day 0), AMPA (*GRIA1,* $P < 0.01$ day 14 and $P < 0.0001$ day 28–35 compared to day 0) and NMDA subunits (*GRIN1,* $P < 0.001$ day 21 and $P < 0.0001$ day 28–35 compared to day 0. GRIN2A, $P < 0.01$ day 21, $P < 0.001$ day 28 and $P < 0.0001$ day 35 compared to day 0. GRIN2B, $P < 0.001$ day 21 and $P < 0.0001$ day 28–35 compared to day 0. GRIN2C, $P < 0.05$ day 28. GRIN2D, $P < 0.05$ day 14, $P < 0.001$ day 21 + 35 and $P < 0.0001$ day 28 compared to day 0) at different stages of neuronal differentiation (mean ± SEM, $n = 3$, $m = 4$). **C/D/E/F:** Change in intracellular calcium oscillations following treatment with C) 10 μM NR2C/NR2D antagonist QNZ46 (QNZ), 10 μM NR2A/NR2B antagonist ketamine (Keta), 10 μM NR2B antagonist TCN237 (TCN), and 10 μM NR2B antagonist ifenprodil (ifen). The vertical black line indicates compound application. D) 10 μM ACh antagonist mecamylamine (Mec), 100 μM GABA antagonist bicuculline (Bicu), and 50 μM NMDA antagonist MK-801, E) 1 μM GABA PAM diazepam (Diaze), and 250 μM AMPA PAM Cx516, F) 10 μM α7 PAM PNU-120596 and 1 μM α7 antagonist MLA, Traces are representative. Data are depicted as mean ± SEM (d36-39, $n = 3$–6, $m = 4$–6). **All figure panels:** Statistical significance was determined using ordinary ANOVA followed by post hoc Dunnett's multiple comparison test; $^{*}P < 0.05$, $^{**}P < 0.01$, $^{***}P < 0.005$.

channel activation.

Intracellular calcium measurements functionally confirmed the nAChR subunits heterogeneity indicated by the qPCR data: Acetylcholine (100 μM) and nicotine (25 μM) treatments induced small increases in intracellular calcium levels, which were strongly amplified by PNU-120596 (3 μM). PNU-282987 (10 μM) alone had no effect, but the signal strongly increased with co-application of PNU-120596 (Fig. 2E). The α7 antagonist, methyllycaconitine (MLA, 1 μM) (Briggs et al., 1995; Macallan et al., 1988) strongly reduced acetylcholine and nicotine signals, while it abolished the PNU-282987 signal (Fig. 2E). The α4β2 antagonist DhβE (1 μM) did not significantly reduce the signal of acetylcholine and nicotine (Fig. 2E). Overall, the pharmacological responses demonstrated nAChR subunits heterogeneity and the presence of functional α7 receptors. To substantiate the pharmacological demonstration of α7 in the hiPSC-derived neuronal cultures, we showed that acetylcholine and PNU-282987 in combination with PNU-120596 (3 μM) resulted in a concentration-dependent increase in intracellular calcium with EC50s of 3 μM and 34 nM, respectively (Fig. 2F). Likewise, a concentration-dependent inhibition was observed with increasing concentrations of MLA (Fig. 2F). Full inhibition of the α7 signal was achieved with 1 μM MLA.

We challenged the system with voltage-gated sodium and calcium channel blockers and inhibitors of intracellular calcium stores to identify the secondary mechanisms of intracellular calcium increase upon α7 receptor activation (Fig. 2 G). Application of TTX (1 μM) and the L-type voltage-gated calcium channel blocker nifedipine (1 μM) reduced the α7 peak amplitude, while no or very minor effects were seen of N-type voltage-gated calcium channel blockers ω-Conotoxin GVIA (1 μM) and ω-Conotoxin MVIIA (1 μM). The ryanodine receptor inhibitor ryanodine caused a border line ($P < 0.05$ with 10 μM) reduction of the α7 peak amplitude, while the inositol trisphosphate receptor inhibitor (IP3), 2-aminoethoxydiphenylborate (2-APB) significantly ($P < 0.0001$) decreased the amplitude in both concentrations tested. This demonstrates influx of extracellular calcium via L-type voltage-gated calcium channel as well as release from intracellular stores.

Stimulating the hiPSC-derived neurons with PNU-120596 (10 μM) combined with PNU- 282987 (10 μM) resulted in increased ERK 1/2 phosphorylation and c-Fos protein expression ($P < 0.05$) (Fig. 2H). As expected, MLA (1 μM) had an antagonizing effect. In line with the data of Fig. 2E, PAM was needed to introduce an effect in these downstream pathways. The ERK 1/2 phosphorylation and c-Fos data reveal that α7 receptor stimulation activates intracellular signaling.

3.3. α7 activation was achieved by type II and intermediate type I/II positive allosteric modulators

Using the paradigm shown in Fig. 2C, we applied a selection of chemically diverse α7 PAMs in combination with PNU-282987. Both type-II PAMs (PNU-120596, TQS), and intermediate type-I/II PAMs (JNJ-39393406, AF58801) resulted in concentration-dependent increases in intracellular calcium, which could be concentration-dependently inhibited by MLA (Fig. 3A).

3.4. Synchronized calcium oscillations in hiPSC-derived neural networks are orchestrated by NMDA and ACh receptors

To assess whether hiPSC-derived neurons could serve as a synaptic transmission model, neural cultures were matured for five weeks. At this point, they contained 96 ± 3% TUJ1 positive neurons and a small population of GFAP positive glia cells 4 ± 3% ($n = 3$, $m = 110$–306, example of image shown in Fig. 4A). The cultures consistently exhibited spontaneous calcium oscillations as described above. Furthermore, they contained chemical synapses signified by positive stains for the presynaptic markers synapsin-1 and vesicular glutamate transporter (Fig. 4A).

Gene expression profiles of selected NMDA, AMPA and GABA receptor subunits showed upregulation of all subunits in hiPSC-derived neurons versus undifferentiated hiPSCs using qPCR (Fig. 4B). The data are in line with the functional neurotransmitter responses (Fig. 1D) supporting the presence of GABA, acetylcholine, and glutamate receptors. NMDA receptors are composed of two NR1 and two NR2 subunits, which can be either subtype A, B, C or D. The strongest increase in NR2 subunit expression was observed for the NR2B subunit (*GRIN2B*, Fig. 4B). We applied four NMDA antagonists with partial selectivity for different NMDA receptor subunits to further investigate the subunit identity (Fig 4E). The NR2A/B antagonist ketamine (10 μM) as well as the NR2B antagonists TCN237 (10 μM) and ifenprodil (10 μM) reduced the calcium oscillation frequency, while the NR2C/D antagonist QNZ46 (10 μM) showed no effect. Collectively, gene expression and calcium oscillation data indicate that a majority of the NMDA receptor complexes are composed of NR2B.

We investigated the effects of NMDA, AMPA, GABA and acetylcholine receptor antagonists or modulators on the frequency and amplitude of the calcium oscillation in the neurons. It should be noted that due to the binding dynamics of the calcium sensitive probe, the two parameters are not completely independent. The NMDA receptor antagonist MK-801 (50 μM) abolished all calcium oscillations (Fig. 4D). Bicuculline (100 μM), a $GABA_A$ receptor antagonist, significantly reduced the peak frequency (0.6 ± 0.03 fold, $P < 0.05$, Fig. 4D). The α7 antagonist mecamylamine (10 μM) significantly reduced peak frequency (0.7 ± 0.1 fold, $P < 0.01$, Fig. 4D). Application of diazepam (Fig. 4C), a $GABA_A$ receptor PAM, showed an increase in frequency (1.7 ± 0.3 fold, $P < 0.05$) and a decrease in amplitude (0.4 ± 0.1, $P < 0.005$). The observed effects of modulating GABA are in line with the observation that GABA is excitatory in the present model (see Section 3.1). The AMPA PAM Cx516 (Fig. 4E) had no significant effects on the tested parameters, although AMPA subunit 1 was upregulated (*GRIA*, day 28, 114 ± 10 fold). This does not exclude the presence of AMPA receptors, but indicate that they do not modulate the calcium oscillations. Overall, the data show NMDA NR2B complex mediated synchronized calcium oscillations and modulation of the synaptic transmission by GABA and acetylcholine receptors.

The α7 receptor has previously been reported to modulate synaptic transmission and ease the threshold for glutamate release in hippocampus and pre-frontal cortex (Alkondon et al., 2000; Alkondon and Albuquerque, 2001; Cheng and Yakel, 2014; Gray et al., 1996;

Sharma et al., 2008). To test the α7 receptors' effect on calcium oscillations in our neuronal network model, we applied PNU-120596 (10 μM) or MLA (1 μM). PNU-120596 resulted in a significant increase in oscillation frequency (1.6 ± 0.2 fold, $P < 0.05$), while MLA had no effect (Fig. 4F). Hence, a positive modulation of α7 intensified the oscillation frequency, while α7 receptor inhibition did not affect the calcium oscillation parameters. This demonstrates the involvement of the α7 receptor in synaptic transmission in the hiPSC neurons.

4. Discussion

Given the interest in the α7 receptor as a target for treatment of cognitive impairment in neurological disease such as Alzheimer's disease and schizophrenia, we used our previously established hiPSC neural culture (Hansen et al., 2016) to study endogenously expressed α7 receptors. Our model system has a good throughput as one 6-well of hiPSCs generates 1200–1600 96-well plates (50.000 cells/well) of neurons(present study and Hansen et al., 2016). The neuronal differentiations of the NSCs were highly reproducible. The hiPSC-derived neurons exhibited neuronal identity as they expressed mRNA and protein for neuronal markers, responded to membrane depolarization,demonstrated expression of functional neurotransmitter receptorsand had synaptic connections and spontaneous calcium oscillations. Hence, the scalability, reproducibility and cellular identity of the model qualifies it for use in pharmaceutical research.

We demonstrated the expression of several different nAChR subunit transcripts in the neuronal cultures indicating the presence of a heterogeneous population of nAChRs. This was functionally confirmed by the pharmacological characterization in the intracellular calcium assay. Potentiation of acetylcholine, nicotine and PNU-282987 by α7 receptor PAM PNU-120596 and inhibition of this potentiation with the α7 antagonist MLA demonstrated the presence of functional α7 receptors. This was substantiated by the presence of concentration-dependent responses to the α7 receptor agonist PNU-282987 in combination with either of four α7 receptor type-I/II or type II PAMs. Moreover, we showed that α7 activation stimulated intracellular signaling in the form of increased c-Fos expression and phosphorylation of ERK 1/2. In line with other α7 receptor studies in mammalian cells, we saw no or very minor effect of agonist alone on intracellular calcium levels, ERK 1/2 phosphorylation and c-Fos expression. This is probably due to the rapid desensitization of α7 nAChR that is induced by orthosteric agonists. Our data also showed that the α7 induced increases in intracellular calcium levels were partly due to influx via the α7 receptor itself, and partly due to calcium influx via voltage-gated calcium channels and release from intracellular stores. This is in line with findings in PC12 (Guerra-Álvarez et al., 2015) and SH-SY5Y cells (Dajas-Bailador et al., 2002a). The fact that the voltage-gated sodium channel inhibitor TTX diminish the signal could points to either reduced opening of voltage-gated calcium channels or reduced axonal signal transmission limiting activation of other subpopulation of neurons not expressing α7 nAChRs. Overall, the α7 receptors in the hiPSC-derived neurons showed the expected pharmacological activation patterns and biologically relevant intracellular signaling and interactions.

Interestingly, the gene expression of TMEM35 was up-regulated during neural maturation and the TMEM35 protein levels in hiPSC-derived neuronal cultures corresponded to levels in PC12 cells. A study has demonstrated TMEM35 to be transiently expressed in the prefrontal cortex of postnatal rats, and that activation of α7 increased TMEM35 protein levels (Wichern et al., 2017). This pattern of co-expression is in agreement with another publication showing TMEM35 to be required for surface localization of α7 and the hetero-pentameric α4β2 nAChRs (Gu et al., 2016). In our study, gene expression levels of TMEM35 also correlated with expression of CHRNA7, CHRNA4, and CHRNB2 mRNA. Consequently, our hiPSC-derived neuronal model is a valid candidate for investigations of TMEM35 and the trafficking dynamics of α7 and other nAChR subunits.

Primary cortical neurons and neurons derived from human embryonic stem cells possess synchronized spontaneous calcium oscillations (Dravid and Murray, 2004; Kiiski et al., 2013). We were among the first to demonstrate synchronized spontaneous calcium oscillations in hiPSC neurons (Hansen et al., 2016; Kirwan et al., 2015). In the current study, we characterize the synaptic transmission driving the network activity. During early embryonic development gap junctions mediate neuronal network activity, while chemical synaptic transmission takes over later in prenatal development (Blankenship and Feller, 2010; Sutor and Hagerty, 2005). Expression of synapsin-1 and vesicular glutamate transporter protein in our neuronal cultures pointed to the presence of chemical synapsis. The effects of NMDA, GABA and acetylcholine receptor antagonists and AMPA and GABA PAMs on the calcium network activity proved roles for NMDA, GABA, and acetylcholine, but not AMDA, neurotransmitters in basal synaptic transmission. In line, we showed gene expression upregulation of the corresponding receptor subunits, and we have previously demonstrated upregulations of the neurotransmitter synthesis rate limiting enzymes, choline acetyltransferase and glutamate decarboxylase 1 (Hansen et al., 2016). Gene expression data in the present study indicated that the larger proportion of the NMDA receptor complexes are composed of NR2B, which may point to a more embryonic NMDA subunit composition (Ewald and Cline, 2009; Zhang and Sun, 2011). Overall, we demonstrate a hiPSC-derived neural network of a relatively advanced neuronal maturity where NMDA, GABA, and acetylcholine signaling mediated synaptic transmission. Our findings add important knowledge to earlier publication on hiPSC-derived neurons investigating exclusively glutamatergic modulation (Kirwan et al., 2015).

Several studies have shown that presynaptic a7 receptors can modulate GABAergic (Alkondon et al., 2000; Alkondon and Albuquerque, 2001) and glutamatergic synaptic transmission in murine hippocampus (Alkondon et al., 2000; Alkondon and Albuquerque, 2001; Gray et al., 1996). Importantly, our human model confirmed involvement of the α7 receptor in synaptic transmission. We show that application of α7 receptor PAM PNU-120596 caused a strong increase in calcium oscillation peak frequency. In contrast to the general nicotinic acetylcholine receptor antagonist mecamylamine, the α7 antagonist MLA had no effects on the oscillation parameters, implying that acetylcholine signaling through the α7 receptor has no prominent effect on basal synaptic activity but rather plays a prominent role for increasing synaptic activity. This opens potential for use of the network activity assay in α7 drug discovery, especially as the fluorescent probe-based assay provides higher throughput than traditional assessments of neuronal network activity (e.g. multi electrode recordings).

5. Conclusions

We have successfully demonstrated that hiPSC can be used to generate a reproducible model system with a throughput that enables its use in pharmacological screening. The neurons could consistently be matured into cultures exhibiting synchronized spontaneous calcium oscillations which were facilitated by NMDA, GABA, and acetylcholine receptors. We clearly demonstrate the presence of functional α7 receptors as early as the second week of neural maturation and showed effect of several type I/II and type II α7 PAMs. We substantiate that our hiPSC-based model is a useful tool for studying pharmacology of endogenously expressed native α7 receptors with relevant cellular functions, as well as for studying receptors implicated in synaptic transmission. Importantly, we demonstrate a role for α7 receptors role in increasing synaptic transmission. We anticipate that such approaches could potentially be used as a phenotypic endpoint in patient-specific hiPSC-based investigations of Alzheimer's disease or schizophrenia.

Declaration of Competing Interest

Tina C. Stummann is employee of Lundbeck.

Acknowledgment

This work was supported by awards from: EU FP7 Marie Curie Industry-Academia Partnerships and Pathways (IAPP) grant (STEMMAD, PIAPP-GA-2012-324451) and Innovation Fund Denmark (BrainStem, 4108-00008B and COGNITO).

Supplementary materials

Supplementary material associated with this article can be found, in the online version, at doi:10.1016/j.scr.2019.101642.

References

Adams, C.E., Broide, R.S., Chen, Y., Winzer-Serhan, U.H., Henderson, T.A., Leslie, F.M., Freedman, R., 2002. Development of the alpha7 nicotinic cholinergic receptor in rat hippocampal formation. Brain Res. Dev. Brain Res. 139, 175–187. https://doi.org/10.1016/S0165-3806(02)00547-3.

Alkondon, M., Albuquerque, E.X., 2001. Nicotinic acetylcholine receptor α7 and α4β2 subtypes differentially control GABAergic input to CA1 neurons in rat hippocampus. J. Neurophysiol. 86, 3043–3055. https://doi.org/10.1152/jn.2001.86.6.3043.

Alkondon, M., Braga, M.F., Pereira, E.F., Maelicke, A., Albuquerque, E.X., 2000. Alpha7 nicotinic acetylcholine receptors and modulation of gabaergic synaptic transmission in the hippocampus. Eur. J. Pharmacol. 393, 59–67. https://doi.org/10.1016/S0014-2999(00)00006-6.

Araud, T., Graw, S., Berger, R., Lee, M., Neveu, E., Bertrand, D., Leonard, S., 2011. The chimeric gene CHRFAM7A, a partial duplication of the CHRNA7 gene, is a dominant negative regulator of α7*nAChR function. Biochem. Pharmacol. 82, 904–914. https://doi.org/10.1016/j.bcp.2011.06.018.

Biton, B., Bergis, O.E., Galli, F., Nedelec, A., Lochead, A.W., Jegham, S., Godet, D., Lanneau, C., Santamaria, R., Chesney, F., Léonardon, J., Granger, P., Debono, M.W., Bohme, G.a., Sgard, F., Besnard, F., Graham, D., Coste, A., Oblin, A., Curet, O., Vigé, X., Voltz, C., Rouquier, L., Souilhac, J., Santucci, V., Gueudet, C., Françon, D., Steinberg, R., Griebel, G., Oury-Donat, F., George, P., Avenet, P., Scatton, B., 2007. SSR180711, a novel selective alpha7 nicotinic receptor partial agonist: (1) binding and functional profile. Neuropsychopharmacology 32, 1–16. https://doi.org/10.1038/sj.npp.1301189.

Blankenship, A.G., Feller, M.B., 2010. Mechanisms underlying spontaneous patterned activity in developing neural circuits. Nat. Rev. Neurosci. 11, 18–29. https://doi.org/10.1038/nrn2759.

Breese, C.R., Adams, C., Logel, J., Drebing, C., Rollins, Y., Barnhart, M., Sullivan, B., Demasters, B.K., Freedman, R., Leonard, S., 1997. Comparison of the regional expression of nicotinic acetylcholine receptor alpha7 mRNA and [125I]-alpha-bungarotoxin binding in human postmortem brain. J. Comp. Neurol. 387, 385–398.

Brennand, K.J., Simone, A., Jou, J., Gelboin-Burkhart, C., Tran, N., Sangar, S., Li, Y., Mu, Y., Chen, G., Yu, D., McCarthy, S., Sebat, J., Gage, F.H., 2011. Modelling schizophrenia using human induced pluripotent stem cells. Nature 473, 221–225. https://doi.org/10.1038/nature09915.

Briggs, C.A., Mckenna, D.G., Piattina-kaplan, M., 1995. Human α 7 nicotinic acetylcholine receptor responses to novel ligands. Neuropharmacology 34, 583–590. https://doi.org/10.1016/0028-3908(95)00028-5.

Chalifoux, J.R., Carter, A.G., 2011. GABAB receptor modulation of voltage-sensitive calcium channels in spines and dendrites. J. Neurosci. 31, 4221–4232. https://doi.org/10.1523/JNEUROSCI.4561-10.2011.

Cheng, Q., Yakel, J.L., 2014. Presynaptic α7 nicotinic acetylcholine receptors enhance hippocampal mossy fiber glutamatergic transmission via PKA activation. J. Neurosci. 34, 124–133. https://doi.org/10.1523/JNEUROSCI.2973-13.2014.

Court, J.A., Lloyd, S., Johnson, M., Griffiths, M., Birdsall, N.J., Piggott, M.A., Oakley, A.E., Ince, P.G., Perry, E.K., Perry, R.H., 1997. Nicotinic and muscarinic cholinergic receptor binding in the human hippocampal formation during development and aging. Brain Res. Dev. Brain Res. 101, 93–105.

Dajas-Bailador, F.A., Mogg, A.J., Wonnacott, S., 2002a. Intracellular Ca 2+ signals evoked by stimulation of nicotinic acetylcholine receptors in SH-SY5Y cells: contribution of voltage-operated Ca2+ channels and Ca2+ stores. J. Neurochem. 81, 606–614. https://doi.org/10.1046/j.1471-4159.2002.00846.x.

Dajas-Bailador, F.A., Soliakov, L., Wonnacott, S., 2002b. Nicotine activates the extracellular signal-regulated kinase 1/2 via the alpha7 nicotinic acetylcholine receptor and protein kinase A, in SH-SY5Y cells and hippocampal neurones. J. Neurochem. 80, 520–530.

Dineley, K.T., Westerman, M., Bui, D., Bell, K., Ashe, K.H., Sweatt, J.D., 2001. β-amyloid activates the mitogen-activated protein kinase cascade via hippocampal alpha7 nicotinic acetylcholine receptors: in vitro and in vivo mechanisms related to Alzheimer's disease. J. Neurosci. 21, 4125–4133. https://doi.org/10.1074/jbc.M200066200.

Dragunow, M., 2008. The adult human brain in preclinical drug development. Nat. Rev. Drug Discov. 7, 659–666. https://doi.org/10.1038/nrd2617.

Dravid, S.M., Murray, T.F., 2004. Spontaneous synchronized calcium oscillations in neocortical neurons in the presence of physiological [Mg2+]: involvement of AMPA/kainate and metabotropic glutamate receptors. Brain Res. 1006, 8–17. https://doi.org/10.1016/j.brainres.2004.01.059.

El Kouhen, R., Hu, M., Anderson, D.J., Li, J., Gopalakrishnan, M., 2009. Pharmacology of alpha7 nicotinic acetylcholine receptor mediated extracellular signal-regulated kinase signalling in PC12 cells. Br. J. Pharmacol. 156, 638–648. https://doi.org/10.1111/j.1476-5381.2008.00069.x.

Eskildsen, J., Redrobe, J.P., Sams, A.G., Dekermendjian, K., Laursen, M., Boll, J.B., Papke, R.L., Bundgaard, C., Frederiksen, K., Bastlund, J.F., 2014. Discovery and optimization of Lu AF58801, a novel, selective and brain penetrant positive allosteric modulator of alpha-7 nicotinic acetylcholine receptors: attenuation of subchronic phencyclidine (PCP)-induced cognitive deficits in rats following oral ad. Bioorganic Med. Chem. Lett. 24, 288–293. https://doi.org/10.1016/j.bmcl.2013.11.022.

Ewald, R.C., Cline, H.T., 2009. NMDA receptors and brain development. In: Van Dongen, A. (Ed.), Biology of the NMDA Receptor. CRC Press/Taylor & Francis, Boca Raton (FL).

Fabian-Fine, R., Skehel, P., Errington, M.L., Davies, H.a., Stewart, M.G., Fine, a., 2001. Ultrastructural distribution of the α7 nicotinic acetylcholine receptor subunit in rat hippocampus. J. Neurosci. 21, 7993–8003 21/20/7993 [pii].

Falk, L., Nordberg, A., Seiger, A., Kjaeldgaard, A., Hellström-Lindahl, E., 2003. Higher expression of alpha7 nicotinic acetylcholine receptors in human fetal compared to adult brain. Brain Res. Dev. Brain Res. 142, 151–160.

Freedman, R., Wetmore, C., Stromberg, I., Leonard, S., Olson, L., 1993. □□a-Bungarotoxin binding to hippocampal interneurons: lmmunocytochemical characterization and effects on growth factor expression. J. Neurosci. 13, 1965–1975.

Gill, J.K., Chatzidaki, A., Ursu, D., Sher, E., Millar, N.S., 2013. Contrasting properties of α7-selective orthosteric and allosteric agonists examined on native nicotinic acetylcholine receptors. PLoS One 8, e55047. https://doi.org/10.1371/journal.pone.0055047.

Gray, R., Rajan, A.S., Radcliffe, K.a., Yakehiro, M., Dani, J.a., 1996. Hippocampal synaptic transmission enhanced by low concentrations of nicotine. Nature 383, 713–716. https://doi.org/10.1038/383713a0.

Grønlien, J.H., Håkerud, M., Ween, H., Thorin-hagene, K., Briggs, C.A., Gopalakrishnan, M., Malysz, J., Halvard, J., Håkerud, M., Ween, H., Thorin-hagene, K., Briggs, C.A., Gopalakrishnan, M., Malysz, J., 2007. Distinct profiles of α7 nAChR positive allosteric modulation revealed by structurally diverse chemotypes. Mol. Pharmacol. 72, 715–724. https://doi.org/10.1124/mol.107.035410.tamers.

Gu, S., Matta, J.A., Lord, B., Harrington, A.W., Sutton, S.W., Davini, W.B., Bredt, D.S., 2016. Brain α7 nicotinic acetylcholine receptor assembly requires nacho. Neuron 89, 948–955. https://doi.org/10.1016/j.neuron.2016.01.018.

Guerra-Álvarez, M., Moreno-Ortega, A.J., Navarro, E., Fernández-Morales, J.C., Egea, J., López, M.G., Cano-Abad, M.F., 2015. Positive allosteric modulation of alpha-7 nicotinic receptors promotes cell death by inducing Ca2+ release from the endoplasmic reticulum. J. Neurochem. https://doi.org/10.1111/jnc.13049. n/a-n/a.

Hajós, M., Hurst, R.S., Hoffmann, W.E., Krause, M., Wall, T.M., Higdon, N.R., Groppi, V.E., 2005. The selective alpha 7 nicotinic acetylcholine receptor agonist PNU-282987 enhances GABAergic synaptic activity in brain slices and restores auditory gating deficits in anesthetized rats. J. Pharmacol. Exp. Ther. 312, 1213–1222. https://doi.org/10.1124/jpet.104.076968.CHRNA7.

Hansen, H.H., Timmermann, D.B., Peters, D., Walters, C., Damaj, M.I., Mikkelsen, J.D., 2007. Alpha-7 nicotinic acetylcholine receptor agonists selectively activate limbic regions of the rat forebrain: an effect similar to antipsychotics. J. Neurosci. Res. 85, 1810–1818. https://doi.org/10.1002/jnr.21293.

Hansen, S.K., Borland, H., Hasholt, L.F., Tümer, Z., Nielsen, J.E., Rasmussen, M.A., Nielsen, T.T., Stummann, T.C., Fog, K., Hyttel, P., 2016. Generation of spinocerebellar ataxia type 3 patient-derived induced pluripotent stem cell line SCA3.B11. Stem Cell Res. 16, 589–592. https://doi.org/10.1016/j.scr.2016.02.042.

Hashimoto, K., Ishima, T., Fujita, Y., Matsuo, M., Kobashi, T., Takahagi, M., Tsukada, H., Iyo, M., 2008. Phencyclidine-Induced cognitive deficits in mice are improved by subsequent subchronic administration of the novel selective α7 nicotinic receptor agonist SSR180711. Biol. Psychiatry 63, 92–97. https://doi.org/10.1016/j.biopsych.2007.04.034.

Haydar, S.N., Dunlop, J., 2010. Neuronal nicotinic acetylcholine receptors - targets for the development of drugs to treat cognitive impairment associated with schizophrenia and Alzheimer's disease. Curr. Top. Med. Chem. 10, 144–152. https://doi.org/10.2174/156802610790410983.

Hurst, R.S., Hajós, M., Raggenbass, M., Wall, T.M., Higdon, N.R., Lawson, J.a., Rutherford-Root, K.L., Berkenpas, M.B., Hoffmann, W.E., Piotrowski, D.W., Groppi, V.E., Allaman, G., Ogier, R., Bertrand, S., Bertrand, D., Arneric, S.P., 2005. A novel positive allosteric modulator of the alpha7 neuronal nicotinic acetylcholine receptor: in vitro and in vivo characterization. J. Neurosci. 25, 4396–4405. https://doi.org/10.1523/JNEUROSCI.5269-04.2005.

Israel, M.a., Yuan, S.H., Bardy, C., Reyna, S.M., Mu, Y., Herrera, C., Hefferan, M.P., Van Gorp, S., Nazor, K.L., Boscolo, F.S., Carson, C.T., Laurent, L.C., Marsala, M., Gage, F.H., Remes, A.M., Koo, E.H., Goldstein, L.S.B., 2012. Probing sporadic and familial Alzheimer's disease using induced pluripotent stem cells. Nature 482, 216–220. https://doi.org/10.1038/nature10821.

Kesselheim, A.S., Hwang, T.J., Franklin, J.M., 2015. Two decades of new drug development for central nervous system disorders. Nat. Rev. 14, 815–816. https://doi.org/10.1038/nrd4793.

Kiiski, H., Aanismaa, R., Tenhunen, J., Hagman, S., Yla-Outinen, L., Aho, A., Yli-Hankala, A., Bendel, S., Skottman, H., Narkilahti, S., 2013. Healthy human CSF promotes glial differentiation of hESC-derived neural cells while retaining spontaneous activity in existing neuronal networks. Biol. Open 2, 605–612. https://doi.org/10.1242/bio.20134648.

Kirwan, P., Turner-Bridger, B., Peter, M., Momoh, A., Arambepola, D., Robinson, H.P.C., Livesey, F.J., 2015. Development and function of human cerebral cortex neural networks from pluripotent stem cells in vitro. Development 142, 3178–3187. https://doi.org/10.1242/dev.123851.

Krause, R.M., Buisson, B., Bertrand, S., Corringer, P.J., Galzi, J.L., Changeux, J.P.,

Bertrand, D., 1998. Ivermectin: a positive allosteric effector of the alpha7 neuronal nicotinic acetylcholine receptor. Mol. Pharmacol. 53, 283–294. https://doi.org/10.1124/mol.53.2.283.

Levin, E.D., Bradley, A., Addy, N., Sigurani, N., 2002. Hippocampal alpha 7 and alpha 4 beta 2 nicotinic receptors and working memory. Neuroscience 109, 757–765. https://doi.org/10.1016/S0306-4522(01)00538-3.

Levin, E.D., McClernon, F.J., Rezvani, A.H., 2006. Nicotinic effects on cognitive function: behavioral characterization, pharmacological specification, and anatomic localization. Psychopharmacology (Berl) 184, 523–539. https://doi.org/10.1007/s00213-005-0164-7.

Lieberman, J.A., Dunbar, G., Segreti, A.C., Girgis, R.R., Seoane, F., Beaver, J.S., Duan, N., Hosford, D.A., 2013. A randomized exploratory trial of an α-7 nicotinic receptor agonist (TC-5619) for cognitive enhancement in schizophrenia. Neuropsychopharmacology 38, 968–975. https://doi.org/10.1038/npp.2012.259.

Macallan, D.R.E., Lunt, G.G., Wonnacott, S., Swanson, K.L., Rapoport, H., Albuquerque, E.X., 1988. Methyllycaconitine and (+)-anatoxin-a differentiate between nicotinic receptors in vertebrate and invertebrate nervous systems. FEBS Lett. 226, 357–363. https://doi.org/10.1016/0014-5793(88)81454-6.

Millan, M.J., Agid, Y., Brüne, M., Bullmore, E.T., Carter, C.S., Clayton, N.S., Connor, R., Davis, S., Deakin, B., DeRubeis, R.J., Dubois, B., Geyer, M.A., Goodwin, G.M., Gorwood, P., Jay, T.M., Joëls, M., Mansuy, I.M., Meyer-Lindenberg, A., Murphy, D., Rolls, E., Saletu, B., Spedding, M., Sweeney, J., Whittington, M., Young, L.J., 2012. Cognitive dysfunction in psychiatric disorders: characteristics, causes and the quest for improved therapy. Nat. Rev. Drug Discov. 11, 141–168. https://doi.org/10.1038/nrd3628.

Muratore, C.R., Rice, H.C., Srikanth, P., Callahan, D.G., Shin, T., Benjamin, L.N.P., Walsh, D.M., Selkoe, D.J., Young-Pearse, T.L., 2014. The familial Alzheimer's disease APPV717i mutation alters APP processing and TAU expression in iPSC-derived neurons. Hum. Mol. Genet. 23, 3523–3536. https://doi.org/10.1093/hmg/ddu064.

Prickaerts, J., van Goethem, N.P., Chesworth, R., Shapiro, G., Boess, F.G., Methfessel, C., Reneerkens, O.A.H., Flood, D.G., Hilt, D., Gawryl, M., Bertrand, S., Bertrand, D., König, G., 2012. EVP-6124, a novel and selective α7 nicotinic acetylcholine receptor partial agonist, improves memory performance by potentiating the acetylcholine response of α7 nicotinic acetylcholine receptors. Neuropharmacology 62, 1099–1110. https://doi.org/10.1016/j.neuropharm.2011.10.024.

Rasmussen, M.A., Holst, B., Tümer, Z., Johnsen, M.G., Zhou, S., Stummann, T.C., Hyttel, P., Clausen, C., 2014. Transient p53 suppression increases reprogramming of human fibroblasts without affecting apoptosis and DNA damage. Stem Cell Rep. 3, 404–413. https://doi.org/10.1016/j.stemcr.2014.07.006.

Selkoe, D.J., 2011. Resolving controversies on the path to Alzheimer's therapeutics. Nat. Med. 17, 1060–1065. https://doi.org/10.1038/nm.2460.

Sharma, G., Grybko, M., Vijayaraghavan, S., 2008. Action potential-independent and nicotinic receptor-mediated concerted release of multiple quanta at hippocampal CA3-Mossy fiber synapses. J. Neurosci. 28, 2563–2575. https://doi.org/10.1523/JNEUROSCI.5407-07.2008.

Sinkus, M.L., Graw, S., Freedman, R., Ross, R.G., Lester, H.A., Leonard, S., 2015. The human CHRNA7 and CHRFAM7A genes: a review of the genetics, regulation, and function. Neuropharmacology 96, 274–288. https://doi.org/10.1016/j.neuropharm.2015.02.006.

Succol, F., Fiumelli, H., Benfenati, F., Cancedda, L., Barberis, A., 2012. Intracellular chloride concentration influences the GABAA receptor subunit composition. Nat. Commun. 3, 738. https://doi.org/10.1038/ncomms1744.

Sutor, B., Hagerty, T., 2005. Involvement of gap junctions in the development of the neocortex. Biochim. Biophys. Acta 1719, 59–68. https://doi.org/10.1016/j.bbamem.2005.09.005.

Takahashi, K., Tanabe, K., Ohnuki, M., Narita, M., Ichisaka, T., Tomoda, K., Yamanaka, S., 2007. Induction of pluripotent stem cells from adult human fibroblasts by defined factors. Cell 131, 861–872. https://doi.org/10.1016/j.cell.2007.11.019.

Thomsen, M.S., Hansen, H.H., Timmerman, D.B., Mikkelsen, J.D., 2010a. Cognitive improvement by activation of alpha7 nicotinic acetylcholine receptors: from animal models to human pathophysiology. Curr. Pharm. Des. 16, 323–343.

Thomsen, M.S., Hay-Schmidt, A., Hansen, H.H., Mikkelsen, J.D., 2010b. Distinct neural pathways mediate α7 nicotinic acetylcholine receptor-dependent activation of the forebrain. Cereb. Cortex 20, 2092–2102. https://doi.org/10.1093/cercor/bhp283.

Timmermann, D.B., Grønlien, J.H., Kohlhaas, K.L., Nielsen, E.Ø., Dam, E., Jørgensen, T.D., Ahring, P.K., Peters, D., Holst, D, Chrsitensen, J.K., Malysz, J., Briggs, C.a., Gopalakrishnan, M., Olsen, G.M., 2007. An allosteric modulator of the α7 nicotinic acetylcholine receptor possessing cognition-enhancing properties in vivo. J. Pharmacol. Exp. Ther. 323, 294–307. https://doi.org/10.1124/jpet.107.120436.vidual.

Toyohara, J., Hashimoto, K., 2010. α7 nicotinic receptor agonists: potential therapeutic drugs for treatment of cognitive impairments in schizophrenia and Alzheimer's disease. Open Med. Chem. J. 4, 37–56. https://doi.org/10.2174/1874104501004010037.

Wichern, F., Jensen, M.M., Christensen, D.Z., Mikkelsen, J.D., Gondré-Lewis, M.C., Thomsen, M.S., 2017. Perinatal nicotine treatment induces transient increases in NACHO protein levels in the rat frontal cortex. Neuroscience 346, 278–283. https://doi.org/10.1016/j.neuroscience.2017.01.026.

Williams, D.K., Wang, J., Papke, R.L., 2011. Positive allosteric modulators as an approach to nicotinic acetylcholine receptor-targeted therapeutics: advantages and limitations. Biochem. Pharmacol. 82, 915–930. https://doi.org/10.1016/j.bcp.2011.05.001.

Yu, J., Vodyanik, M.A., Smuga-Otto, K., Antosiewicz-Bourget, J., Frane, J.L., Tian, S., Nie, J., Jonsdottir, G.A., Ruotti, V., Stewart, R., Slukvin, I.I., Thomson, J.A., 2007. Induced pluripotent stem cell lines derived from human somatic cells. Science 318, 1917–1920. https://doi.org/10.1126/science.1151526.

Zhang, Z., Sun, Q.-Q., 2011. Development of NMDA NR2 subunits and their roles in critical period maturation of neocortical GABAergic interneurons. Dev. Neurobiol. 71, 221–245. https://doi.org/10.1002/dneu.20844.